The Application of SSC for RFI Suppression in SLC Images of Sentinel-1 IW Mode

Yueli Sun, Hengrui Zhang, Bingxu Chen, Gaofeng Shu, and Ning Li, *Member, IEEE*

***Abstract*— Synthetic aperture radar (SAR) images of Sentinel-1 (S-1) in interferometric wide (IW) swath mode, which are widely used for land and ocean services, but are affected by severe radio frequency interference (RFI). Single look complex (SLC) data containing phase and amplitude information is the most popular product type for SAR applications. The sub-band spectral cancellation (SSC) method extracts and suppresses RFI in SLC images by making a subtraction among different sub-images, which is efficient and strong enough to be applied to projects based on the hypothesis that the range spectrum is particularly symmetric. However, through the theoretical analysis of the imaging algorithm for generating SLC data in S-1 IW mode, it is found that the phase compensation step in the azimuth post-processing destroys the symmetry of the spectrum and does not meet the basis for the application of the SSC method, resulting in poor RFI mitigation performance. Based on this discovery, inverse phase compensation is first performed on the RFI-contaminated SLC image to restore the spectrum symmetry. The second step is the sub-band division and sub-image energy cancellation. This method effectively protects useful signals while suppressing RFI, which is significantly essential for the further application of S-1 SLC images. The availability of the method has been proved by simulated and measured experiments.**

***Index Terms*— Radio frequency interference (RFI) suppression, Sentinel-1 (S-1) Satellite, single look complex (SLC), sub-band spectral cancellation (SSC), synthetic aperture radar (SAR), terrain observation by progressive scans SAR (TOPSAR).**

I. Introduction

SENTINEL-1 (S-1) satellite's active sensing element of synthetic aperture radar (SAR) working in the C-band is able to track the ground at any time during the day or night, no matter how the climate or atmosphere is [1]. S-1 provides different-level products with open access. The level-1 products called single look complex (SLC) working in interferometric wide (IW) mode, S-1 satellite's primary acquiring mode, containing not only amplitude but also phase information, have wide application in a large number of domains. However, according to the public report, SLC images are affected by radio frequency interference (RFI), which can be seen in Fig. 1, bringing bad effects to certain essential applications. Hence, it is necessary and significant to find a method for RFI suppression in SLC SAR images of S-1 IW mode.

Over some previous periods, various RFI suppression methods have emerged, which are separated into three kinds, including parametric, semi-parametric, and nonparametric methods [2]. The parametric method is realized by constructing a precise math model so that RFI suppression will be changed to a parameter assessment issue. Similarly, the semi-parametric methods change the complex signal separation to a hyperparameter improvement issue, utilizing an optimization model to constrain and separate RFI. According to sparse and low-rank characteristics, the RFI optimization model is first founded and then used for RFI suppression. Nonparametric method, instead of building a mathematical model of RFI, blindly separates RFI and useful signals by transforming the signal into different domains. The mainstream methods include time-domain notch filtering (TNF) [3], and 2-D notch filter [4], [5], which are used to a great extent because of easy enforcement and high calculational effectiveness. Moreover, another popular type of nonparametric method extracts and suppresses RFI by matrix disintegration, such as robust principal component analysis (RPCA) [6], and eigen-subspace projection (ESP) [7].

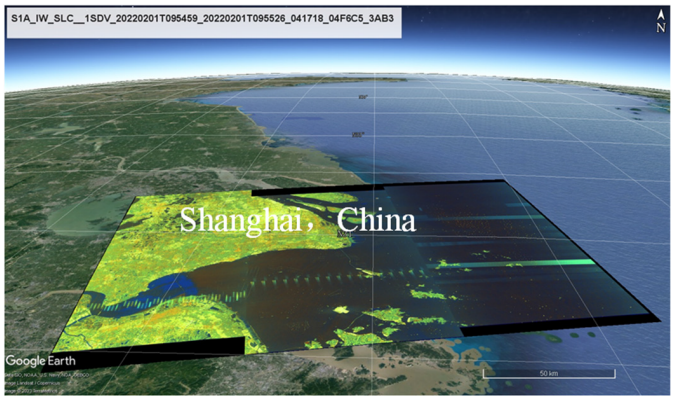

Fig. 1. RFI-contaminated Sentinel-1 SAR data illuminated area.

Unlike the above-mentioned methods, which are primarily used for level-0 products (raw data), the sub-band spectral cancellation (SSC) method is a nonparametric method [8] for level-1 products (SLC) on account of the premise that the range spectrum is precisely symmetrical. In traditional stripmap mode, range spectrum is purely symmetric, which is also the basis for the application of the SSC method. However, in the IW mode utilizing terrain observation with progressive scans SAR (TOPSAR), beams are controlled from back to front by electronic means in azimuth orientation for all bursts [9]. For this reason, the problem of spectrum aliasing and time aliasing needs to be solved by pre-processing and post-processing operations in the processing algorithm, in which the phase compensation step destroys the symmetry of the spectrum and does not meet the basis for the application of the SSC method, resulting in inferior RFI mitigation performance.

To solve the problem, an RFI suppression strategy specific to SLC data in S-1 IW mode, namely inverse phase

Manuscript received 29 May 2023; revised 7 October 2023; accepted 12 October 2023. Date of publication 16 October 2023; date of current version 25 October 2023. This work was supported by Natural Science Foundation of Henan under Grant 222300420115. *(Corresponding author: Gaofeng Shu.)*

The authors are with the College of Computer and Information Engineering, the Henan Key Laboratory of Big Data Analysis and Processing, and the Henan Province Engineering Research Center of Spatial Information Processing, Henan University, Kaifeng 475004, China (e-mail: gaofeng.shu@henu.edu.cn).

Digital Object Identifier 10.1109/LGRS.2023.3324803

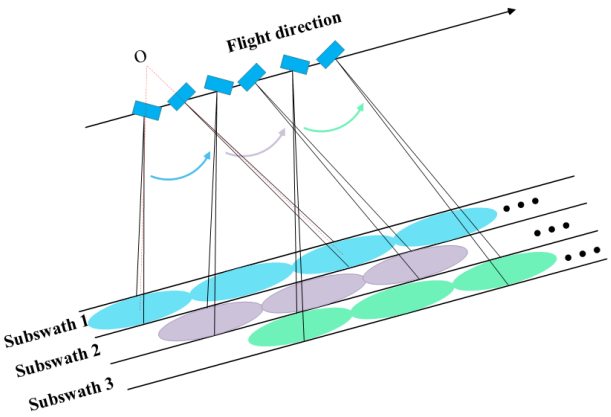

Fig. 2. TOPSAR geometric model.

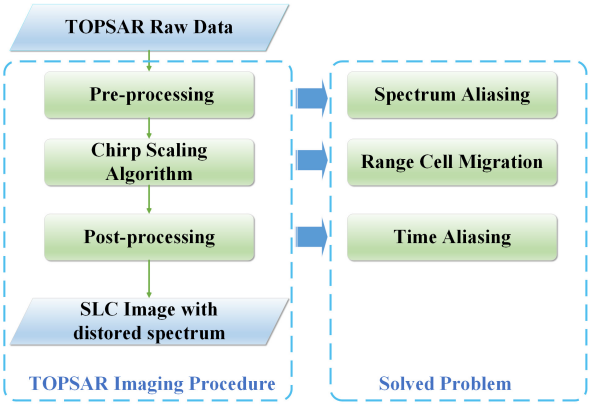

Fig. 3. TOPSAR imaging procedure.

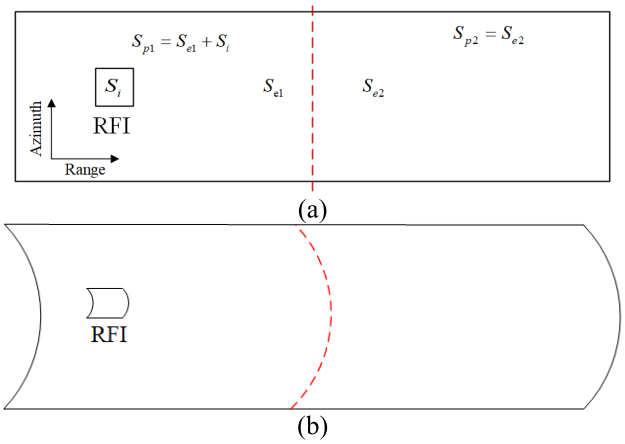

Fig. 4. (a) Diagram of symmetry spectrum. (b) Diagram of distorted spectrum.

compensation, is proposed to restore the spectrum symmetry caused by the imaging algorithm in the ground processor. After that, the second step of traditional SSC can be performed. According to the symmetrical range spectrum, signals with and without RFI are divided into different sub-bands. Finally, the energy of corresponding sub-images can be canceled, maintaining the image free of RFI. This method can effectively protect useful signals while suppressing RFI, which improves RFI mitigation performance and has significant value for the future application of S-1 SLC images. The effect of the suggested method is displayed by simulated and measured experiments.

The following is the arrangement of this letter. In Section II, first of all, the background of the problem is introduced in Part A; next, the rule of the SSC method is introduced in Part B; finally, the problem is analyzed in Part C. The methodology of the problem is described in Section III. Simulated and S-1 SLC experiment results are displayed in Section IV. At last, the letter is briefly summarized in Section V.

II. Problem Statement

A. Background of the Problem

SLC images of S-1 IW mode are obtained in TOPSAR mode, whose geometric model is shown in Fig. 2. TOPSAR overcomes the scalloping effect while acquiring the same range-wide swath as ScanSAR by actively scanning the beam in azimuth orientation and periodically adjusting beam angle in range orientation. Because of this special working mode, it is not enough to just use the traditional CS algorithm in the stripmap mode. Fig. 3 revealed that the S-1 SLC imaging procedure in IW mode extends the imaging capability of adding azimuth pre-processing measures to settle the aliased Doppler spectrum and post-processing measures to unfold the back-folded SAR image [10].

Through the analysis of the imaging procedure, it is found that the phase compensation in the last step of post-processing destroys the symmetry of the spectrum, as shown in Fig. 4(b), which is the basis of the SSC method. Therefore, the problem of spectrum asymmetry should be resolved.

B. Basis of the SSC Method

The SSC method fully uses the holography of SAR imaging, spectrum symmetry, and features of RFI in the frequency domain, realizing RFI detection and elimination for the image products through range frequency spectrum division [11]. In detail, the SSC method relies upon the unique spectrum characteristic of RFI and useful SAR signals. The narrow-band RFI signals commonly situate at some frequency in the unsymmetric spectrum. In contrast, the spectrum of the SAR signal is commonly symmetric. What's more, the sub-band signals can be imaged separately. With the SSC method, the symmetric SAR signals can be removed, and the unsymmetric RFI signals can be obtained.

In order to elaborate on the basis of SSC specifically, two sub-bands are taken as an example, which is also applicable to multiple sub-bands. Without considering the noise, since the RFI signal and target signal are independent of each other, the received echo signal can be modeled as follows:

$$S_p = S_e + S_i \tag{1}$$

where S_p, S_e, and S_i represent the original whole data, useful data, and RFI-contaminated data in time domain, separately.

After FFT in range direction, RFI is detected in the range-frequency domain through the average range spectrum algorithm [12]. The spectrum is separated into two symmetrical sub-band spectrums containing RFI and not, which is shown in Fig. 4(a). The two sub-bands can be expressed as

$$S_{p1} = S_{e1} + S_i \tag{2}$$

$$S_{p2} = S_{e2}. \tag{3}$$

In which S_{p1} and S_{p2} represent two sub-bands in time domain, separately; S_{e1} and S_{e2} represent two sub-bands not containing RFI in the time domain, separately.

After spectrum correction processing, the amplitude of the sub-band signal is approximately the same. After this operation, following equation can be obtained, showing the symmetry of the spectrum:

$$|S_{e1}|^2 - |S_{e2}|^2 \approx 0. \tag{4}$$

C. Problem Analysis

The spectrum shown in Fig. 4(b) clearly illustrates the problem of spectrum distortion in S1-SLC images caused by phase compensation. In the last step of post-progressing, after phase compensation is performed in the time domain, multiplying the phase, the signal can be transformed into

$$S_n(\tau, \eta) = S_p(\tau, \eta) \cdot \exp\left(-j\pi K \tau^2\right). \tag{5}$$

In which η and τ refer to the azimuth slow time and the range fast time separately. $S_p(\tau, \eta)$ and $S_n(\tau, \eta)$ refer to the data before and after phase compensation. K refers to the Doppler modulation rate. After Fourier transformation, the spectrum of the signal will be described as

$$S_n(f, \eta) = \int_{-\tau/2}^{\tau/2} S_n(\tau, \eta) \exp(-j2\pi f \tau) d\tau \tag{6}$$

where $S_n(\tau, \eta)$ represent signals that vary in the time domain, and $S_n(f, \eta)$ refers to its equivalent frequency-domain result after the Fourier transform. f is frequency. Substituting $S_n(\tau, \eta)$ in (6) with (5), the spectrum can be obtained after derivation

$$S_n(f, \eta) = S_p\left(\frac{f}{K}\right) \exp\left(-j\pi \frac{f^2}{K}\right). \tag{7}$$

According to the property of Fourier transformation in the time domain, the signal multiplied by the phase information in the time domain is equivalent to the spectrum shift in the frequency domain. From the formula (7), we can see that the relationship between the spectrum and the frequency is quadratic and curved, obviously breaking the symmetry of the spectrum. Therefore, a symmetrical spectrum cannot be obtained because of the phase compensation operation, so the energy of the divided sub-bands (S_{e1} and S_{e2}) is unequal. That is to say, (4) is no longer equal. From the principle of the SSC method introduced in part B, it is clear that the realization of the sub-band division step is to obtain a symmetrical sub-band spectrum by dividing the range spectrum equally in the frequency domain according to the symmetric features of the range spectrum. However, the basis of the traditional SSC method is no longer satisfied, which hinders the correct implementation of the subsequent sub-band energy cancellation operation, thereby significantly reducing RFI suppression performance.

III. Methodology

For the purpose of solving above-mentioned problems and improving RFI suppression capabilities, this letter proposes a method. It is extremely necessary to perform Inverse Phase Compensation first to restore its spectral symmetry characteristic and then perform traditional SSC [8] to suppress RFI signals. The first step is the innovative part in order to restore the spectrum symmetry. The second part is inherited from the traditional SSC method. The flow diagram of the suggested method is displayed in Fig. 5.

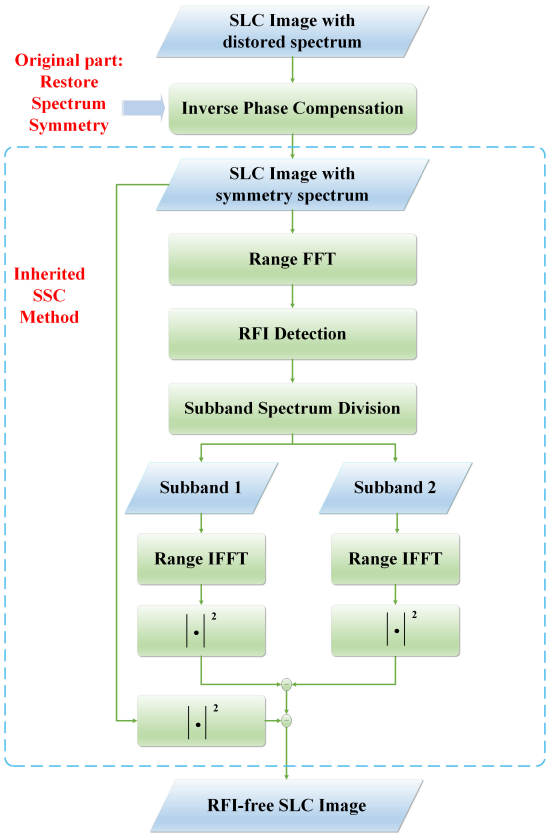

Fig. 5. Flowchart of the proposed methodology.

A. Inverse Phase Compensation

In the process of TOPSAR imaging, the phase compensation operation destroys the symmetry of the spectrum and affects the effect of SSC RFI suppression. Therefore, performing inverse phase compensation first is extremely important to restore its spectrum symmetry. The Inverse Phase Function can restore the distorted spectrum, which is described as

$$S_p(\tau, \eta) = S_n(\tau, \eta) \cdot \exp\left(j\pi K \tau^2\right) \tag{8}$$

where $S_p(\tau, \eta)$ and $S_n(\tau, \eta)$ represent focused image data with a symmetrical spectrum and a distorted spectrum.

B. Sub-Band Spectrum Division

After obtaining a symmetrical spectrum, the signals can be divided into sub-bands with and without RFI according to the average distance spectrum method and then returned to the time domain through Range IFFT to obtain sub-images [8]. Apparently, the whole power spectrum of sub-image will be described as

$$\left|S_{p1}\right|^2 \approx |S_{e1}|^2 + |S_i|^2 \tag{9}$$

$$\left|S_{p2}\right|^2 \approx |S_{e2}|^2. \tag{10}$$

C. Sub-Image Energy Cancellation

The energy of the sub-images can be obtained by subtracting the energy of the sub-image to obtain the power of the RFIs and then suppressing the power of the RFIs from the power of the whole image [8]. The image without RFI can be obtained. The following formula explains this process in detail.

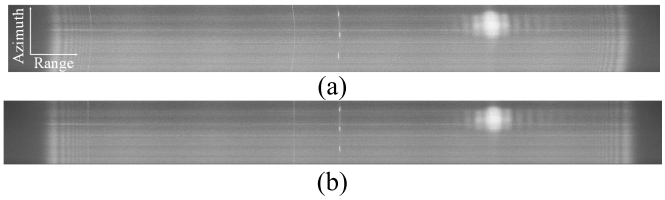

Fig. 6. (a) Spectrum before inverse phase compensation. (b) Spectrum after inverse phase compensation.

Make subtraction between (9) and (10)

$$\left|S_{p1}\right|^2 - \left|S_{p2}\right|^2 \approx |S_{e1}|^2 - |S_{e2}|^2 + |S_i|^2. \tag{11}$$

After replacing (11) with (4), RFIs will be got

$$\left|S_{p1}\right|^2 - \left|S_{p2}\right|^2 \approx |S_i|^2. \tag{12}$$

To sum up, no RFI-contaminated signal S_e will be got

$$|S_e|^2 = \left|S_p\right|^2 - |S_i|^2 = \left|S_p\right|^2 - \left|\left|S_{p1}\right|^2 - \left|S_{p2}\right|^2\right|. \tag{13}$$

Contrasted with the conventional SSC method, the main improvement of this method is that it restores the spectrum symmetry by inverse phase compensation, effectively reducing energy loss while suppressing RFI.

IV. Experiment Results

For the purpose of demonstrating the validity of the suggested method, the RFI simulation experiment and measured experiment were carried out, respectively. RFI mitigation experiment outcomes are displayed in the figures below.

A. RFI Simulation Results

The spectrum before and after the phase compensation operation is displayed in Fig. 6. The measured SAR data added with simulated RFI signals under different SINRs are used to quantitatively analyze the interference suppression results of the proposed method. The measured data is the SLC data of Shanghai on October 23, 2022, obtained from S-1 satellite of the European Space Agency (ESA). Its parameters of the measured data and interference simulation are displayed in Table I. In order to accurately compare different methods and prove the availability of the suggested method, measurable analysis was carried out by the root mean square error (RMSE), which was defined as

$$\mathrm{RMSE}\left(S_{\text{RFI-free}}, S_p\right) = \frac{\left\|S_p - S_{\text{RFI-free}}\right\|_F}{\left\|S_p\right\|_F} \tag{14}$$

where $\|\cdot\|$ denotes the Frobenius norm, S_p denotes original SAR data and $S_{\text{RFI-free}}$ denotes RFI-free SAR data. The contrast between the primary image with RFI and the image after RFI suppression is revealed in RMSE. The lower the RMSE, the more excellent the RFI suppression result.

Fig. 7 shows the variation of RMSE under different SINRs using the traditional SSC method and the proposed method. It can be clearly seen that the RMSE obtained by the proposed method is smaller than that of the traditional SSC method, which proves the effectiveness of the proposed method.

B. Measured Data Experimental Results

Fig. 8 displays the original image using S-1 data and RFI suppression effects. The original data is SLC data of Hangzhou on October 26, 2020, acquired by the S-1 satellite of the ESA, as displayed in Fig. 8(a). Moreover, Fig. 8(b) shows

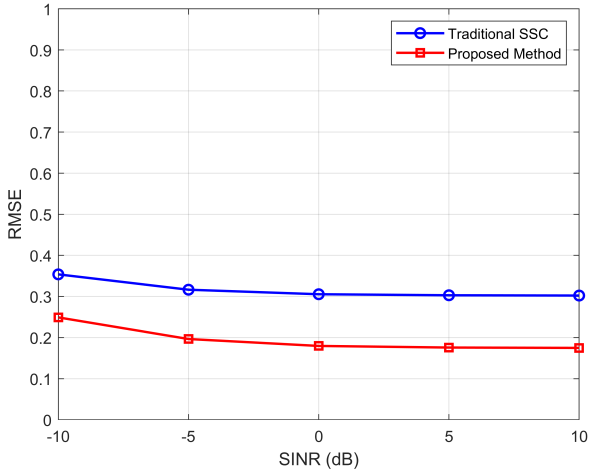

Fig. 7. RMSEs in the case of different SINRs by traditional SSC and proposed method.

TABLE I
Main Simulation Parameters

Parameters	Values
Slant range	800 Km
Pulse width	52.4 μs
Carrier frequency of RFI signal	5.405 GHz
Carrier frequency	5.4 GHz
Bandwidth of RFI signal	2.3 MHz
Sampling frequency	64.3 MHz
Pulse bandwidth	56.6 MHz
Efficient velocity	7184.7 m/s
PRF	1717 Hz

the effect of using traditional SSC for RFI suppression. It can be seen that while the RFI is suppressed, the useful signal is also severely lost. The experimental results of RFI suppression using the method proposed in this letter are displayed in Fig. 8(c). Compared with Fig. 8(b), the useful signal has been protected, which strongly proves the effectivity of the method suggested by the letter. Fig. 8(d)–(g) are enlarged images of the ROI labeled by red and green boxes on Fig. 8(a)–(c), from which the changes in the images can be seen more clearly, representing four different areas: mountain and forest area, urban area, airport area and agricultural area.

For the purpose of measurably evaluating the effectivity of the suggested method, suppression results are analyzed with image entropy [13] and average gradient (AG) [14]. Image entropy indicates information quality of the image. For an image without interference, larger image entropy represents more information and richer geographic information the image includes. AG indicates the ratio at which the comparison of small particulars of the image varies and depicts the comparative clarity of an image. Higher AG represents more layers the image has, and the clearer it is. The analysis outcomes of four different scenes are displayed in Table II. The AG and image entropy of the method suggested in this letter are higher than those of traditional SSC, which further shows the effectiveness of the proposed method.

C. Discussion

Undoubtedly, the SSC method has great engineering value in the field of RFI suppression for SLC images. However,

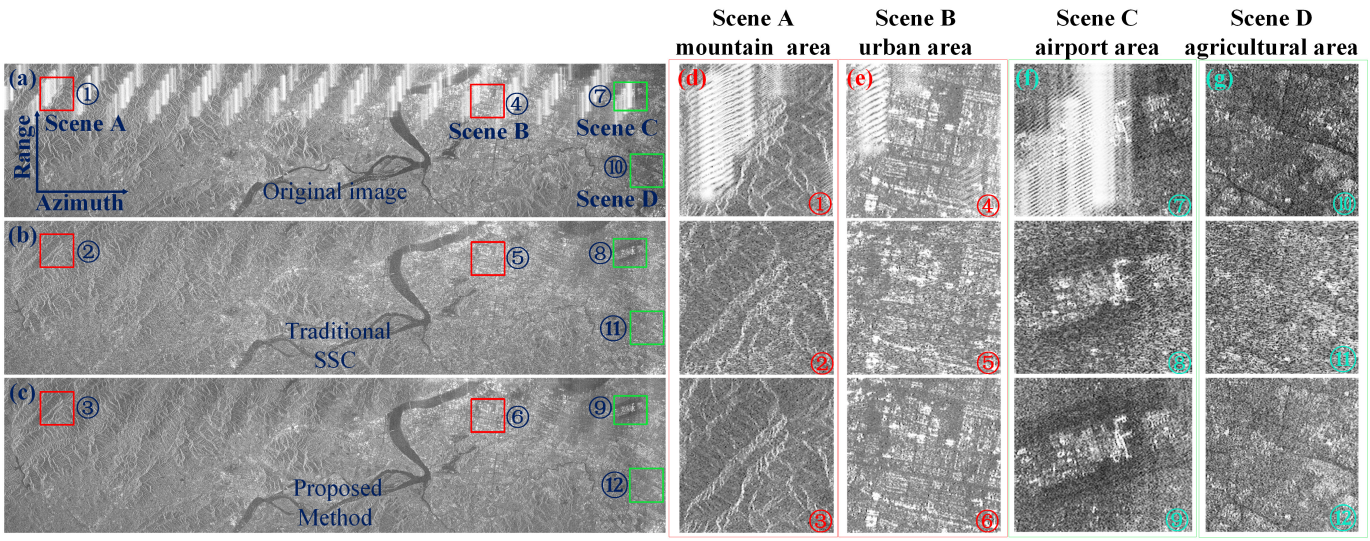

Fig. 8. Experimental results for measured data. (a) Initial imaging result before suppression. (b) Suppression result via conventional SSC method. (c) Suppression result via proposed method. (d)–(g) ROIs in (a)–(c) with red and green box.

TABLE II
EVALUATION METRICS OF DIFFERENT RFI MITIGATION METHODS

Method	Image Entropy				Average Gradient			
	A	B	C	D	A	B	C	D
Traditional SSC	7.5572	7.5423	7.4868	7.4415	1143	1242	1077	1091
Proposed Method	7.6314	7.6754	7.6342	7.7001	1267	1320	1226	1329

for TOPSAR images, the distortion of the spectrum during the imaging process leads to energy loss in the RFI suppression process. The proposed method solves these problems by effectively reducing energy loss, protecting useful signals, and improving the RFI suppression performance of the SSC method. Furthermore, the proposed method demonstrates its effectiveness in different scenes when applied to SLC images. It is worth noting that the proposed method specifically addresses the problem of spectrum asymmetry and is unnecessary for data that does not exhibit spectrum distortion characteristics in other imaging modes, except for TOPSAR mode.

V. CONCLUSION

RFI seriously affects the quality of the S-1 SLC image and hinders its application. The SSC method can efficiently achieve RFI suppression, but the assumption that the spectrum is symmetrical is not satisfied in SLC images of S-1 IW mode. This letter analyzes the S-1 SLC image processing algorithm, the principle of the SSC method, and spectrum symmetry in detail, finding the reason is phase compensation. On this basis, a method to improve the SSC suppression performance is provided, which has great potential in the RFI suppression for SLC images of S-1 and other satellites using TOPSAR mode in the future, addressing an essential issue for SLC image users.

REFERENCES

[1] Q. Lyu et al., "SAR interference suppression algorithm based on low-rank and sparse matrix decomposition in time–frequency domain," *IEEE Geosci. Remote Sens. Lett.*, vol. 19, pp. 1–5, 2022.

[2] M. Tao, J. Su, Y. Huang, and L. Wang, "Mitigation of radio frequency interference in synthetic aperture radar data: Current status and future trends," *Remote Sens.*, vol. 11, no. 20, p. 2438, Oct. 2019.

[3] N. Li, Z. Lv, Z. Guo, and J. Zhao, "Time-domain notch filtering method for pulse RFI mitigation in synthetic aperture radar," *IEEE Geosci. Remote Sens. Lett.*, vol. 19, pp. 1–5, 2022.

[4] Z. Fu, H. Zhang, J. Zhao, N. Li, and F. Zheng, "A modified 2-D notch filter based on image segmentation for RFI mitigation in synthetic aperture radar," *Remote Sens.*, vol. 15, no. 3, p. 846, Feb. 2023.

[5] Y. Cai et al., "First demonstration of RFI mitigation in the phase synchronization of LT-1 bistatic SAR," *IEEE Trans. Geosci. Remote Sens.*, vol. 61, 2023, Art. no. 5217319.

[6] J. Su, H. Tao, M. Tao, L. Wang, and J. Xie, "Narrow-band interference suppression via RPCA-based signal separation in time–frequency domain," *IEEE J. Sel. Topics Appl. Earth Observ. Remote Sens.*, vol. 10, no. 11, pp. 5016–5025, Nov. 2017.

[7] F. Zhou, R. Wu, M. Xing, and Z. Bao, "Eigensubspace-based filtering with application in narrow-band interference suppression for SAR," *IEEE Geosci. Remote Sens. Lett.*, vol. 4, no. 1, pp. 75–79, Jan. 2007.

[8] J. Feng, H. Zheng, Y. Deng, and D. Gao, "Application of subband spectral cancellation for SAR narrow-band interference suppression," *IEEE Geosci. Remote Sens. Lett.*, vol. 9, no. 2, pp. 190–193, Mar. 2012.

[9] A. Meta, J. Mittermayer, P. Prats, R. Scheiber, and U. Steinbrecher, "TOPS imaging with TerraSAR-X: Mode design and performance analysis," *IEEE Trans. Geosci. Remote Sens.*, vol. 48, no. 2, pp. 759–769, Feb. 2010.

[10] W. Xu, P. Huang, R. Wang, Y. Deng, and Y. Lu, "TOPS-mode raw data processing using chirp scaling algorithm," *IEEE J. Sel. Topics Appl. Earth Observ. Remote Sens.*, vol. 7, no. 1, pp. 235–246, Jan. 2014.

[11] A. Reigber and L. Ferro-Famil, "Interference suppression in synthesized SAR images," *IEEE Geosci. Remote Sens. Lett.*, vol. 2, no. 1, pp. 45–49, Jan. 2005.

[12] W. Xu, W. Xing, C. Fang, P. Huang, and W. Tan, "RFI suppression based on linear prediction in synthetic aperture radar data," *IEEE Geosci. Remote Sens. Lett.*, vol. 18, no. 12, pp. 2127–2131, Dec. 2021.

[13] N. Li, Z. Lv, and Z. Guo, "SAR image interference suppression method by integrating change detection and subband spectral cancellation technology," *Syst. Eng. Electron.*, vol. 43, no. 9, pp. 2484–2492, Sep. 2021.

[14] J. Su, H. Tao, M. Tao, J. Xie, Y. Wang, and L. Wang, "Time-varying SAR interference suppression based on delay-Doppler iterative decomposition algorithm," *Remote Sens.*, vol. 10, no. 9, p. 1491, Sep. 2018.